

Behavior of Steel Plate Shear Walls Subjected to Repeated Synthetic Ground Motions

Ramla K. Qureshi, S.M.ASCE¹; and Michel Bruneau, F.ASCE²

Abstract: Steel plate shear walls (SPSWs) have been shown capable of remaining stable under seismic loading due to their satisfactory hysteretic performance. However, since the thin steel web infills within these walls only yield under tension and in most cases exhibit no significant compressive resistance, their behavior is uncertain under long duration of shaking. The scope of this research was to investigate whether there is a point in time where the SPSW behavior becomes that of its own bare frame when subjected to extensive shaking, which would indicate that the steel web plates no longer contribute to response. In this parametric study, SPSWs of various configurations were analyzed using nonlinear inelastic dynamic analyses, for which response modification factor and duration of repetitive synthetic ground motions were varied. Two single-story SPSWs (with panel aspect ratios of 1:1 and 2:1) and one 3-story SPSW (having panel aspect ratio of 1:1) were modeled using the commonly used diagonal strip model. Spectra-compatible synthetically generated ground motions were used in the analyses. SPSW responses were then compared against those of their respective boundary frames. Performance of SPSW over the duration of the repeated stochastic ground motions was characterized by inelastic and residual drifts. The objective of this research was to provide an understanding of the expected ductile performance of SPSWs when subjected to prolonged seismic excitation, and hopefully, an improved confidence in their seismic behavior under such conditions. DOI: 10.1061/(ASCE)ST.1943-541X.0002281. © 2019 American Society of Civil Engineers.

Introduction

Steel plate shear wall (SPSW) systems typically consist of thin, unstiffened vertical steel web panels bounded by a steel boundary frame of horizontal and vertical structural members, respectively called horizontal boundary elements (HBEs) and vertical boundary elements (VBEs). The steel plate web is characteristically relatively thin [generally ranging from 4.75 to 12.5 mm (3/16 to 1/2 in.) in midrise buildings], and, as a consequence of this slenderness, buckles under compression during earthquake loading and an inclined tension field action develops. As such, the web panel shear strength is effectively that provided by the diagonal tension field stresses oriented approximately 45° to the direction of shear loading.

While it has been proven in past research that this tension-only yielding behavior of the infill, in combination with the plastic hinging that develops at the ends of the HBEs, provides SPSWs with adequate seismic performance (e.g., Driver et al. 1998b; Rezai 1999; Astaneh-Asl 2001; Cao et al. 2007; Park et al. 2007; Dastfan and Driver 2008; Choi and Park 2009; Borello et al. 2014; Clayton et al. 2016), it remains that the infill only significantly dissipates hysteretic energy when in tension, and can only do so at tensile strains larger than those previously reached (much like braces do in tension-only braced frames, which are typically not permitted in severe seismic regions). Even though the postbuckling strength and ductility of the infill panel is substantial

(e.g., Elgaaly et al. 1993; Bruneau and Bhagwagar 2002; Berman and Bruneau 2003; Sabouri-Ghomi et al. 2005; Anjan et al. 2009; Berman 2011; Borello and Fahnestock 2013), reliance on this tension-only behavior to achieve satisfactory seismic performance raises legitimate questions regarding the expected behavior of SPSWs during long-duration earthquakes. For example, if the steel web plate can conceptually only stretch once within a cycle at a given drift, how will it contribute adequate hysteretic energy dissipation as ground-motion excitation progressively becomes longer? Will the slack web plate under compression lead to excessive progressively increasing drift, which would negate the objective of using SPSW with high elastic stiffness to limit drift? Likewise, how far will an SPSW drift before its steel webs no longer contribute and response of the system is driven by the stiffness of the SPSW's boundary frame alone? This can be critical when a low-stiffness boundary frame is present, which can occur when steel plate webs of similar thicknesses are used across stories, effectively eliminating the unbalanced force from the yielding webs above and below an HBE that is used in their capacity design [an arbitrary requirement that the SPSW's boundary frame alone be able to resist by 25% of the specified seismic forces, in absence of the SPSW webs, was added to ANSI/AISC 341 (AISC 2016) and CSA S16-14 (CSA 2014) in response to this concern].

This paper presents results from research conducted to better understand the behavior of SPSWs as ground excitation progressively gets longer, to determine if there might be a time during ground motions when the steel web plates cease to contribute to structural response, leaving the system to behave as if it were just the boundary frame, and perhaps have significant consequences in seismic performance. Given that the objective is to understand how SPSWs behave as duration increases, in light of the fact that their primary energy-dissipating elements (the steel webs) behave as a tension-only system, two important simplifications were essential for the analyses.

First, increasing the duration of the ground motions had to be done without modifying the signature of the ground motions, so

¹Graduate Research Assistant, Dept. of Civil, Structural and Environmental Engineering, Univ. at Buffalo, Amherst, NY 14260 (corresponding author). Email: ramlakar@buffalo.edu

²Professor, Dept. of Civil, Structural and Environmental Engineering, Univ. at Buffalo, 130 Ketter Hall, Buffalo, NY 14260. Email: bruneau@buffalo.edu

Note. This manuscript was submitted on March 29, 2018; approved on September 6, 2018; published online on January 24, 2019. Discussion period open until June 24, 2019; separate discussions must be submitted for individual papers. This paper is part of the *Journal of Structural Engineering*, © ASCE, ISSN 0733-9445.

that differences observed could be entirely attributed to differences in SPSW behavior over time, not differences in earthquake characteristics. This is why focus here is on repeated synthetic ground motions, *not* long-duration actual ground motion that would bring up issues of variations in amplitude, frequency content, pulses, fling, relationship of magnitude to peak ground acceleration (PGA), and many others—briefly touched upon in the next section. All these issues are important and investigating their impact on the seismic performance of SPSW would be instructive, but is a topic left for future research.

Second, infinitely ductile response had to be assumed. It is recognized (e.g., Driver et al. 1998b; Qu et al. 2008; Choi and Park 2011; Clayton et al. 2016) and understood that the infills of SPSWs will develop fracture at drifts exceeding 3%, and the strength degradation may also occur from other causes, but, again, considering limit states other than ductile response would prevent acquiring the understanding necessary to address the previous behavior-related questions. Therefore, here, research focused on identifying fundamental behavior and response on the basis of idealized elastic–perfectly plastic material models having infinitely ductile behavior alone to provide an understanding of the factors that would affect ductile response alone (i.e., studying the role of the tension-only webs on response in the best conditions when all other limit states could be prevented). This required that the effects of strain hardening, progressive fracture of the steel web panel from the boundary frame, local buckling of the boundary frame members, P -delta effects, and other failure modes leading to strength degradation and possible collapse be *purposely* ignored for this fundamental study. Even though it is understood that these aspects of behavior and important limit states can potentially affect the behavior of SPSWs, can have a large influence on the effectiveness of the system as a whole during cyclic inelastic response at large and increasing drifts, and/or can lead to their collapse (Purba and Bruneau 2015), it was necessary to ignore these effects to achieve the intended goals for this study because introducing other limit states in the material models would have led to the introduction of various other failure modes and response would have been impacted by multiple strength-degradation conditions, thereby making it impossible to singly explain the stable performance of SPSWs under seismic excitation, despite the fact that their infill plate exhibits pure tension-only behavior.

In other words, the results discussed here look only into the response of SPSWs having idealized tension-only behavior of the steel plate and idealized plastic behavior of the boundary frame when subjected to repeated synthetic ground motions—which is a most important step to better understand the fundamental seismic behavior of SPSWs, the respective role of the steel webs and boundary frame in driving this response, and how their respective roles change during the length of seismic excitation. Once this is established, it would be worthwhile to research the changes in results if SPSW damage models (Purba and Bruneau 2015) are considered. Groundwork from this study can lead to future investigative studies that compare behavior with and without the previously mentioned degradation effects.

Drift results presented throughout this study serve to relatively measure and compare seismic response over time, and to quantify the influence of the plate's tension-only behavior. Residual drifts also serve the same purpose, and should not be considered in an absolute sense.

Scope

The performance of SPSW systems when subjected to prolonged seismic excitation has not been investigated in the past.

As described previously, although understanding the special impact on structural response of various characteristics inherent to actual long-duration earthquakes (like excitation amplitude and frequency content) is not the focus of this research, it is worth recognizing that the effects of long-duration ground motions on structural steel systems have been investigated by numerous researchers for more than 50 years. Early on, Housner (1965), Trifunac and Brady (1975), Vanmarcke and Lai (1980), Kawashima and Takahashi (1985), and Xie and Zhang (1988) determined that ground-motion duration was critical for quantifying structural damage. Many studies [such as Marsh and Gianotti (1994)] performed multiple analyses for high-magnitude, prolonged, synthetic time histories and reported considerable increase in dissipated hysteretic energy (and therefore damage) with increasing duration of ground motion. Steel structures were included in such past studies. For example, Tirca and Tremblay (2004) reported structural failure due to large deformations and development of beam plastic hinges in 8- and 12-story zipper concentrically braced steel frames under several load reversals owing to the long duration of strong ground motion. Likewise, Lignos et al. (2011) established the properties of a power law to relate fracture due to low cycle fatigue in high-rise steel buildings to the energy dissipated during long-period, long-duration shaking, and Chandramohan et al. (2016) calculated a significant increase in the collapse probability of a 5-story steel special moment frame when subjected to long-duration ground shaking. More generally, other studies have investigated the effect of an increased number of cycles on specific aspect of response, such as low-cycle fatigue damage in reinforced concrete frame buildings (Mantawy and Anderson 2018), or the effect of long-duration, long-period ground motion from various perspectives ranging from studies of the global structural response of idealized elastoplastic structures (e.g., Iervolino et al. 2006; Kojima and Takewaki 2015; Hou and Qu 2015, 2016) to that of strength-degrading structural systems (e.g., Bommer et al. 2004) up to multidisciplinary studies of the full potential catastrophic effects of megathrust earthquakes, such as the M9 Project (University of Washington 2018), whose scope includes addressing the response of buildings (e.g., Marafi et al. 2016) to subduction earthquakes.

All of the preceding studies holistically address the special characteristics of long-duration earthquakes, which is valuable and important but beyond the intent here. As indicated in the introduction, the primary objective here is to investigate the fundamental behavior of ideally ductile SPSWs to determine how they can possibly achieve satisfactory seismic response throughout seismic excitations given that the tension-only hysteretic behavior of the infill plate is believed to dominate this hysteretic response. This is achieved by using progressively longer synthetic ground motions.

To investigate this question, a parametric study was conducted for two single-story SPSWs (with panel aspect ratios of 1:1 and 2:1) and a 3-story SPSW (having panel aspect ratio of 1:1) subjected to synthetic ground motions artificially made longer for the sake of observing how behavior of the SPSW would progressively change. The previously mentioned aspect ratio is based on centerline dimensions of the boundary frame elements. The SPSW configurations considered were analyzed using nonlinear inelastic dynamic analyses of the commonly used diagonal strip model that captures the hysteretic behavior of these walls. For perspective, SPSW responses were also compared against those of their respective boundary frames acting alone. The full time history of select responses is provided to explain the key aspects of response observed in this study, and performance of SPSW over the duration of the shaking is characterized by inelastic and residual drifts.

Generation of Stochastic Ground Motions

Nonlinear time-history analyses were conducted to investigate the performance of SPSWs during long-duration ground shaking. For this purpose, spectra-compatible synthetic ground accelerations for Site Class B soils (ASCE 2010) in San Francisco were generated from the Response Spectrum Compatible Time Histories (RSCTH) program (Papageorgiou and Halldorsson 2004). To provide a target for generating the synthetic ground motions, a 5% damped target response spectrum was generated using parameters obtained from the USGS Seismic Design Maps tool (USGS 2014). For Site Class B soils, the short period S_{MS} and the 1-s period S_{M1} spectral accelerations were found as $1.50g$ and $0.649g$, respectively. For the design-basis earthquake (DBE), the design spectral acceleration parameters S_{DS} and S_{D1} were $2/3$ of the preceding values, and were therefore $1.0g$ and $0.432g$, respectively. Fig. 1 shows the design response spectrum (generated by the US Seismic Design Map tool) as an input for the RSCTH code. The program has a parameter called “duration switch, *idurpm*,” which employs the duration model for California (Atkinson and Silva 2000) to calculate ground-motion duration from the prescribed real moment magnitude M_w , and the prescribed real epicentral distance from source to site in kilometers. RSCTH allows for user input for duration of desired acceleration time history, which can then be increased by increasing the number of input time steps, dt , multiplied to the number of data points, nt . Five ground motions, representing earthquakes of duration (D) representative of what would be expected for earthquake magnitudes (M) ranging from 5 to 9, expressed as DM5, DM6, DM7, DM8, and DM9, were generated, with values of PGA of $0.573g$, $0.536g$, $0.525g$, $0.499g$, and $0.485g$, respectively.

These ground motions had total durations of 9, 12, 19, 42, and 116 s, respectively; and 6.82, 8.73, 14.30, 30.53, and 88.05 s bracketed durations, respectively [bracketed duration is defined by Kawashima and Aizawa (1989) as the interval between first and last exceedance of ground acceleration above $\pm 0.1g$]. These ground motions are presented in Fig. 2, while Fig. 3 shows the resulting spectral matching with DBE target spectrum for all synthetic records. Analyses were performed for three SPSW archetypes, designed per different response modification factors and subjected to the previous ground motions of various durations. Besides analyzing for individual ground motions, time-history sequences with twice, thrice, or six times repetition of DM5 and DM8 accelerations were also considered to observe the incremental

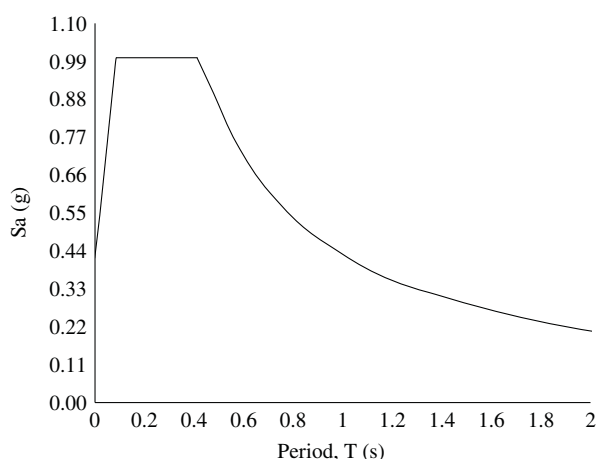


Fig. 1. Design response spectrum.

plastic deformations and residual drifts of SPSWs under prolonged seismic loading. Once again, these stochastic motions are not representative of real earthquakes, and only vary in their bracketed durations.

SPSW Archetype Design and Development of Analytical Models

Two 3.657 m (12 ft)–high, single-story SPSW models were developed with aspect ratios of 1:1 and 2:1, respectively, assumed to be in buildings situated on Site Class B soils (ASCE 2010) in San Francisco. A 3-story, 10.97 m (36 ft)–high wall was also taken into consideration for comparison purposes. The aspect ratio of each of the three infill plates within this wall was taken as 1:1. As indicated in Fig. 4, these walls were labeled as SPSW1, SPSW2, and SPSW3, whereas the bare boundary frames analyzed for comparing response were labeled as MRF1, MRF2, and MRF3, respectively. The bare frames here consist of the boundary elements alone (without the infill plates), instead of moment frames designed to resist the same loads. This was done for reasons that will become more obvious when comparing the responses.

Lateral seismic forces obtained for design have been calculated according to the equivalent lateral force procedure from ASCE 7, Section 12.8 (ASCE 2010). The overstrength factor Ω_o , importance factor I , and deflection amplification factor C_d for the SPSW were defined as 2, 1, and 6, respectively. The approximate fundamental period of the structure, T_o , calculated based on ASCE 7 provisions, was 0.13 s for the single-story archetypes with SPSWs having 1:1 and 2:1 aspect ratios, and 0.35 s for the multistory SPSW archetype considered. Both of these periods fell on the constant-acceleration zone of the design spectra.

The design base shear for each SPSW archetype was calculated as per two different values of response modification factor, R . ASCE 7 specifies the value of R factor that should be used for the design of SPSW. However, because R is related to the level of inelastic demand to be developed in a structural system, SPSWs were designed for values of R of 7 and 5. For SPSW design, per ANSI/AISC 341 (AISC 2016), the web plates designed resist 100% of the specified base shear. For preliminary design the angle of tension stress action, α was assumed to be 45° , and the design strength of the steel plate web panels was calculated per ANSI/AISC 341 Eq. F5-1

$$\phi V_n = 0.90(0.42)F_y t_w L_{cf} \sin(2\alpha)$$

where L_{cf} = clear distance between column flanges; and t_w = thickness of steel plate web (both in inches). In order to design an SPSW with infill plate thickness similar to what is found in applications where hot-rolled plates are used, it was decided to provide a minimum web thickness value, $t_w = 3/16$ in. (4.75 mm). Large values of mass were therefore applied to each wall, and seismic weights were taken as 6,700 kN (1,500 kips), 11,120 kN (2,500 kips), and 26,700 kN (6,000 kips) for SPSW1, SPSW2, and SPSW3, respectively.

The steel web plates were ASTM A36 (ASTM 2014) material, whereas ASTM A992 (ASTM 2015) Grade 50 steel was taken for the boundary frame elements, with nonlinear stress-strain behavior for both materials modeled as elastic–perfectly plastic. Because the drift demand could not be estimated for this study where response under extremely long duration ground motions was to be investigated, the plastic plateau for each material model was assumed constant up to extremely large strains. Figs. 5(c and d) depict the simplified hysteretic behavior of both materials used, with respective values of yield strength $\sigma_y = 248$ MPa (36 ksi) for steel plate

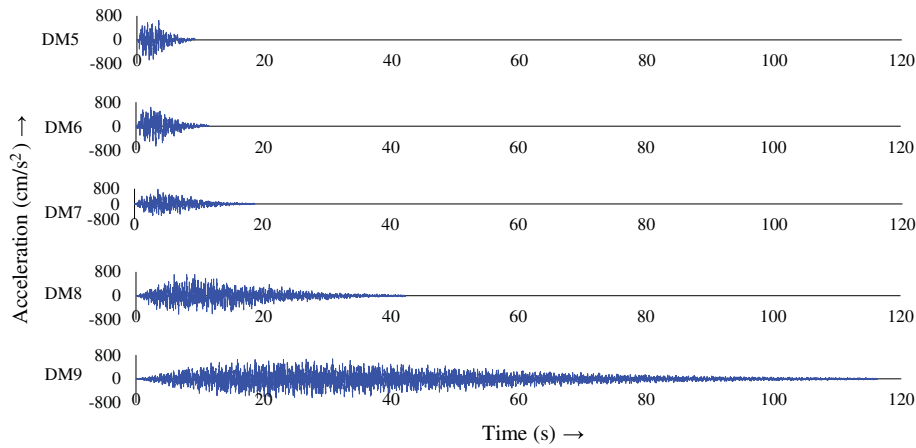


Fig. 2. RSCTH-generated acceleration time histories.

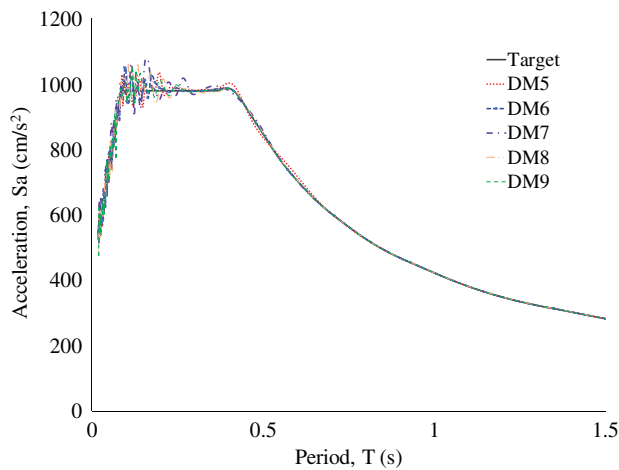


Fig. 3. Spectral matching for synthetic ground motions with target spectrum.

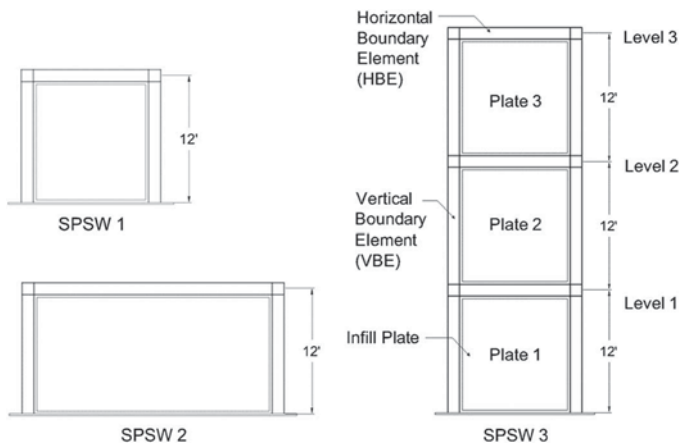


Fig. 4. SPSW archetypes.

and 345 MPa (50 ksi) for boundary elements. The dual-strip model used in this study provides a simple, practical, and validated way to correctly analytically capture the fundamental behavior of SPSWs. For nonlinear pushover analyses, using elastoplastic strips and HBE plastic hinges has been shown to adequately capture the full

force-displacement behavior and ultimate strength of SPSWs, and of their individual stories (e.g., Berman and Bruneau 2004, 2005; Driver et al. 1998a, b; Qu et al. 2008). Previous research has also shown that the strip model can adequately capture the hysteretic behavior of SPSWs provided that a symmetric layout of tension-only strips is used (e.g., Elgaaly et al. 1993; Elgaaly and Liu 1997; Lubell et al. 2000; Qu et al. 2008). For example, Qu et al. (2008) demonstrated this for a full-scale 2-story SPSW specimen subjected to pseudodynamic testing, where using a dual-strip tension-only nonlinear model with 15 strips in each direction provided hysteretic story shear–displacement behavior that accurately matched the experimental results. The same model has been used here, and in much of the contemporary research on SPSW. Each of the archetypes was designed with the expectation that plastic hinges would form at the ends of the HBE near the face of columns, and that the web plates would yield under tension. Capacity design was used to ensure that yielding remained confined to the deformation-controlled elements and that the VBEs and connections have sufficient strength to remain elastic (Berman and Bruneau 2008). Resulting web plate thicknesses and member sizes for HBEs and VBEs for the archetypes are presented in Table 1.

The steel plates were modeled in the program SAP2000 using the dual-strip model proposed by Thorburn et al. (1983), transforming the solid steel panels into parallel, pin-ended tension-only diagonal strips that serve as an equivalent for the tension field action, yielding only in tension and buckling under compression. These strips were expected to load up to yield strength under tension, follow the plastic plateau during the course of continued tension loading, unload until tension was reduced to zero as the seismic loading reversed direction, and exhibit no strength as soon as the plate underwent compression. They are also modeled to unbuckle and return to their longer stretched length prior to reloading in tension. Axial P hinges were assigned at the center of each of the strips to model this nonlinear hysteretic behavior (Purba and Bruneau 2015). For example, Fig. 5(a) shows the hinge numbers assigned to each axial strip for SPSW1, ranging from 5 to 27. This hinge only allows for yielding caused by axial loads. For the strips to mimic actual behavior of the web panels, these axial hinges were assigned compression limits set to zero. For SAP2000 to follow the previously mentioned simplified elastoplastic stress-strain model, some modifications had to be made. The model was designed to log values of the positive residual axial deformation upon unloading as it enters the compression loading regime, and to require the strips to recover all displacements up to the previously recorded positive residual axial deformation value before reloading into the

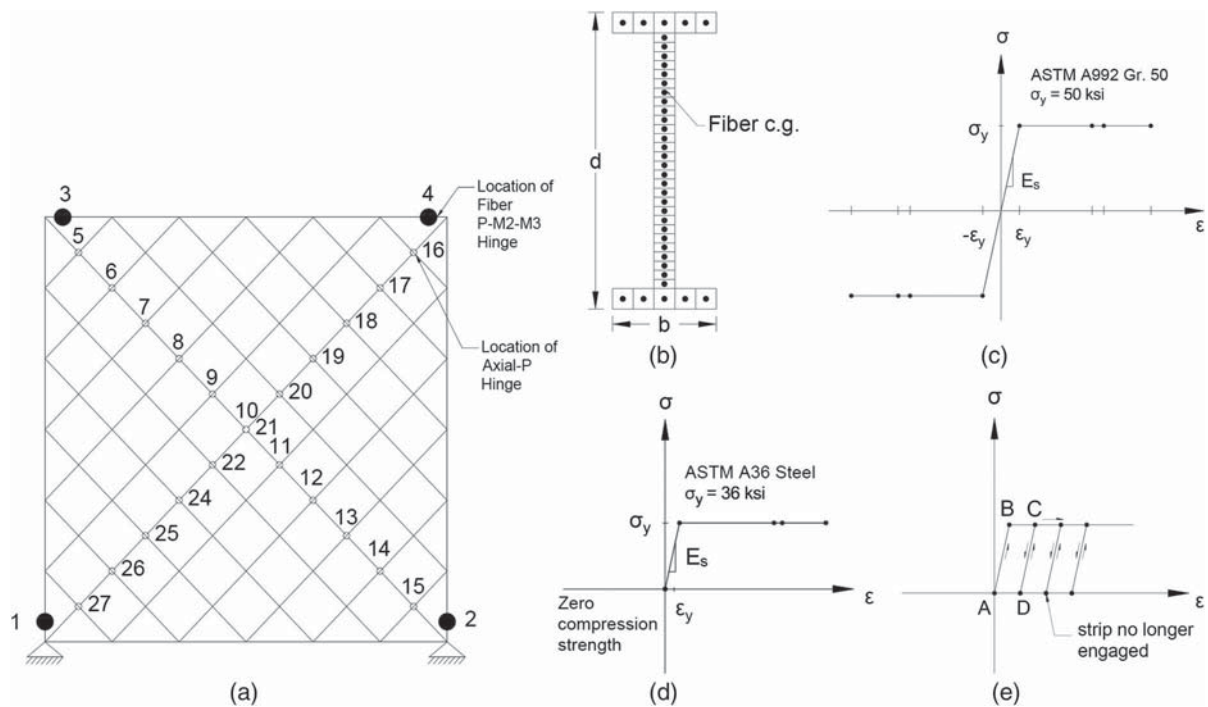


Fig. 5. (a) SPSW1 archetype with axial and fiber hinge locations; (b) location of 38 fibers placed within the HBE cross section; (c) simplified hysteretic material model for flexure; (d) simplified tension-only material model for strips emulating the web plate; and (e) generic strip hysteretic behavior.

Table 1. SPSW web plate thickness and HBE and VBE sizes

Wall	R value	Story	Panel aspect ratio	Plate thickness [mm (in.)]	HBE	VBE
Single story	5	—	1:1	4.75 (3/16)	W40 × 327	W40 × 593
SPSW2	5	—	2:1	4.75 (3/16)	W40 × 431	W36 × 652
Multistory	7	First	1:1	12.5 (1/2)	W40 × 199	W40 × 431
		Second	1:1	11.1 (7/16)	W40 × 199	W40 × 431
		Third	1:1	12.5 (1/2)	W40 × 149	W40 × 324

tension regime again. Fig. 5(e) depicts the corresponding generic hysteretic behavior for the strips. A validation was conducted by applying a nonlinear time-history load case using a cosine function of amplitude 1. The axial hinge was confirmed to only engage during the tension regime of the forcing function and to exhibit tension-only behavior. For example, during the hysteretic response, the first cycle followed the load-displacement path from Point A to Point B, yielding at B, and displacing along the elastic-perfectly-plastic backbone plateau until Point C. Upon reversal, it then unloaded until Point D, from where it underwent further compression while developing no compressive force. Tracking the displacement history revealed that no compressive stress developed within the diagonal strip. Upon load reversal, the strip was only reengaged in tension when its axial deformation returned to Point D, then up to the exact same value of deformation at Point C, where the previous tension regime had ended, and further yielded in tension from there on.

Plastic hinge properties in the boundary frame elements were modeled using Fiber P-M2-M3 hinges. In such hinges, the cross sections for the HBEs and VBEs were divided into layers (i.e., fibers) in both strong and weak directions, with each fiber associated

with its own stress-strain relationship depending on the properties of the material at the corresponding location in the cross section. A total of 38 fibers were modeled for the flexural hinges within the HBE. Fiber locations within the HBE cross sections are depicted in Fig. 5(b). Here, Fibers 2, 4, 34, 36, and 38 are in the top flange; Fibers 1, 3, 5, 35, and 37 are in the bottom flange; and the remaining fibers are located in the web. Of these web fibers, 20–33 are above the neutral axis, whereas 6–19 are located below it (for which numbering is sequential from bottom to top).

Comparative Analyses

For this parametric study, trends in response for the considered SPSWs were observed by varying different parameters, namely, the panel aspect ratios, value of R factor, damping ratio ζ , number of stories, and the duration of the synthetic ground motions. Time-history sequences with twice, thrice, or six times repetition of DM5 and DM8 were also considered, and the following observations were made.

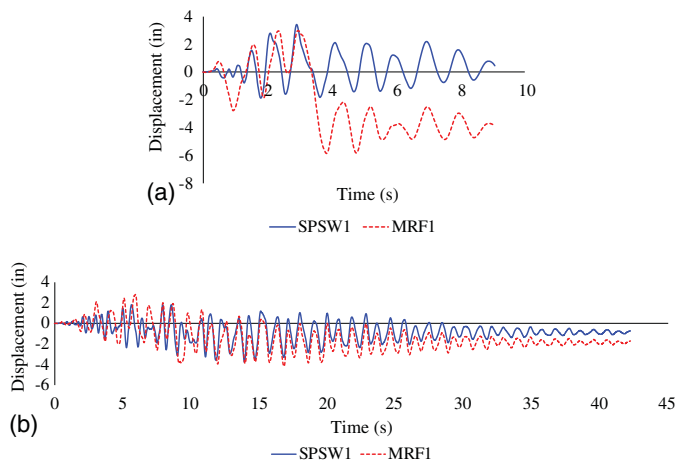


Fig. 6. Drift response for SPSW1 compared with that of MRF1 for (a) DM5; and (b) DM8.

Drift Response

Nonlinear time histories of the SPSW and moment resisting boundary frame (MRF) response were compared in order to detect if there was a point in time where the SPSW infill plates ceased to contribute to the system, and the system response matched that of its respective bare frame as duration of seismic excitation increased. Fig. 6 shows the HBE lateral displacement response of SPSW1 compared to that of MRF1 for duration magnitudes of DM5 and DM8. As was expected, owing to its lesser stiffness, the MRF experienced comparatively larger values of displacement; for example, 147.3 mm (5.8 in.) compared to 86.4 mm (3.4 in.) for SPSW displacement for DM5 magnitude ground motion. The synthetically generated ground-motion time histories obtained from the program RSCTH for lesser durations had to match the same target spectra as those for the longer durations (9 s for DM5 in comparison with 42 s for DM8), leading to low values of peak ground accelerations for the higher-magnitude records, which in turn resulted in values of maximum drift observed for the smaller-magnitude stochastic ground motions to be greater than those for the larger-magnitude ones. This can be observed from Fig. 6 where, for DM5, MRF1 experienced 147.3 mm (5.8 in.) of displacement, as compared to only 100.3 mm (3.95 in.) for the DM8 record. As a result, smaller-magnitude accelerations suffered much more severe yielding even though these had much smaller duration, which is an illogical outcome when comparing actual earthquakes of different magnitudes that would have proportionally different response spectra, but a logical inconsistency introduced by scaling all artificial ground motions to match the same target spectra irrespective of magnitude or duration. For the purpose of this research, it was therefore illogical to make comparisons based on magnitude alone. These results confirmed that in order to observe the effects of long duration, comparisons should be made between synthetic records having similar peak ground accelerations, but with varying duration of ground motion. Therefore, a simple approach taken to study the effects of prolonged seismic loading on SPSW archetypes was to repeat the same ground motion a number of times. This is described further in subsequent sections.

Residual Drifts

Comparing the trace of the response histories, some trends in behavior were observed. For example, a certain sequence of peaks in the SPSW1 displacement histories was observed to appear

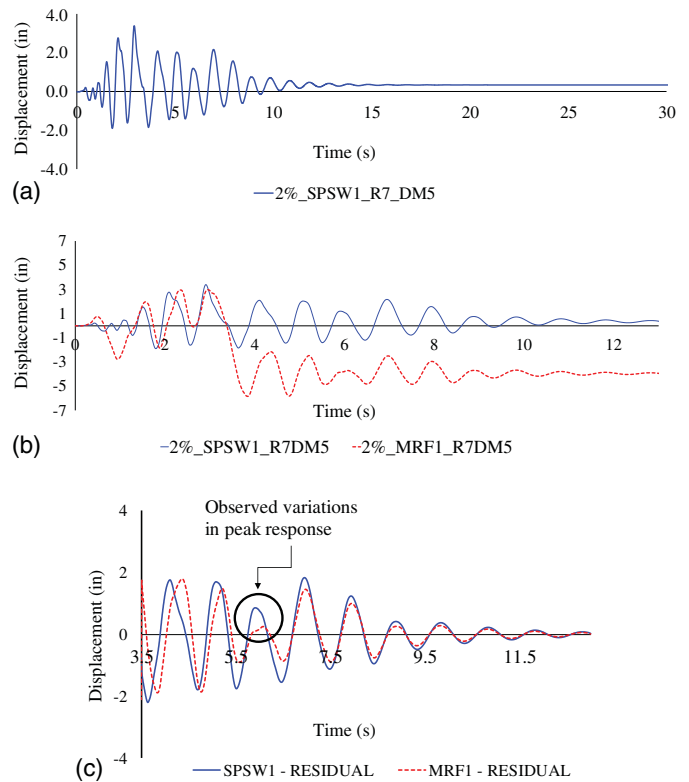


Fig. 7. Displacement response for $R = 7$, DM5: (a) SPSW1 with 20 s of zero padding; (b) SPSW1 and MRF1; and (c) residual displacement subtracted from both responses.

similar to those for MRF1, except for a visible difference caused by the accumulation of residual drift. Subtracting the respective plastic residual displacements from the total response histories for both SPSW1 and MRF1 resulted in curves that could be superimposed to determine if similarities in behavior existed. However, as shown in Fig. 7, the peaks obtained as a result of this procedure did not completely overlay each other, showing variations in both amplitude and shape of the response histories for both archetypes. This variation in response was (expectedly) caused by the presence of the steel infill plate within the SPSW.

Hinge Hysteretic Response

To further investigate the respective contribution of the infill and boundary frame on response, it was decided to study as a function of time the hysteretic behavior of the flexural fiber P-M2-M3 hinges assigned to the HBES in both archetypes within SAP2000. Displacements were considered for quantifying response rather than drifts in order to directly correlate loading and unloading of hinges with the lateral displacement of the wall. Instances in time when the fibers experienced yielding were extracted, and the points when the first and last fibers in these hinges underwent yielding, for the very first and the very last time, were used to define a bracket of time that limits the occurrence of inelastic response during the entire response history. Similarly, for the axial P hinges, all intervals during which the strips underwent plastic yielding for the first and last time were obtained by extracting their force-displacement output data. The results were then plotted with respect to time, effectively mapping the internal yield behavior of both the SPSW and MRF archetypes. The three input ground motions considered for this purpose were:

- DM5: Acceleration time history DM5 with total duration of 9 s;
- DM5+5: Twice the preceding input acceleration with 4 s worth of intermittent zero padding before and after the second consecutive DM5 ground motion, increasing the total duration under consideration to 26 s; and
- DM5+5+5: Similarly increased ground acceleration history, but this time by sequencing three times the original DM5 time history with zero padding at the end of each repetition, for a total duration of 39 s.

Figs. 8(a and b) present the top HBE lateral displacement response with the points of observed yielding for the axial and fiber hinges (marked with respect to time) for the DM5+5+5 repetition, where for the axial hinges, the notations $AHFF_i$ and $AHFL_i$ correspond to the first and last yield point for the *first* axial hinge to yield, and $AHLF_i$ and $AHLL_i$ denote the first and last yield point for the *last* axial hinge that experienced yielding, respectively. Similarly for the case of fiber hinges in both the SPSW and the MRF, the notations used were $FHFF_i$ and $FHFL_i$ for the first and last yield point for the *first* fiber in a fiber hinge to yield, and $FHLF_i$ and $FHLL_i$ for the first and last yield point for the *last* fiber in a fiber hinge that experienced yielding, respectively. The subscript i here referred to the number of times the input time history was repeated to increase duration of loading. For this figure, $i = 1$ to 3.

Fig. 8(a) shows that the first fiber in the MRF1 fiber hinge yielded at a value of $FHFF_1 = 0.81$ s, whereas it can be seen from Fig. 8(b) that the first fiber for the SPSW1 hinge yielded at around

1.71 s. Therefore, a noticeable delay was seen for the first fiber within the SPSW1 HBE fiber hinges to begin plastic behavior compared to those in the MRF1 archetype. This was because, in SPSW1, the axial hinges (conforming to expectation) underwent plastic yielding first at a value of $AHFF_1 = 0.58$ s, limiting drift and delaying involvement of the flexural hinges. Moreover, the last flexural fiber to begin yielding within the SPSW was observed to engage at a much earlier time as compared to the last fiber for the MRF flexural hinge, i.e., at a value of $FHLF_1 = 2.01$ s for SPSW1, as compared to 3.6 s for MRF1. Therefore, it was concluded that the entire HBE cross section within the SPSW fully yielded ahead of the MRF cross section. There was a possibility that this was due to the interaction of the axial force within the SPSW system.

Contribution of the Steel Infill Plate

To check the previously mentioned prospect, three states were noted for the response of each axial hinge, namely, the onset of yielding, the onset of unloading, and the duration between these points during which the hinge follows the constant plastic backbone for the material model defined previously. A bar chart was used to plot all three states with respect to time, where the length of the bar indicated the extent of time for which the considered hinge yielded plastically. Fig. 9 presents a better visual correlation between response and duration of loading by overlaying these yield bars with the displacement histories for each of the three input

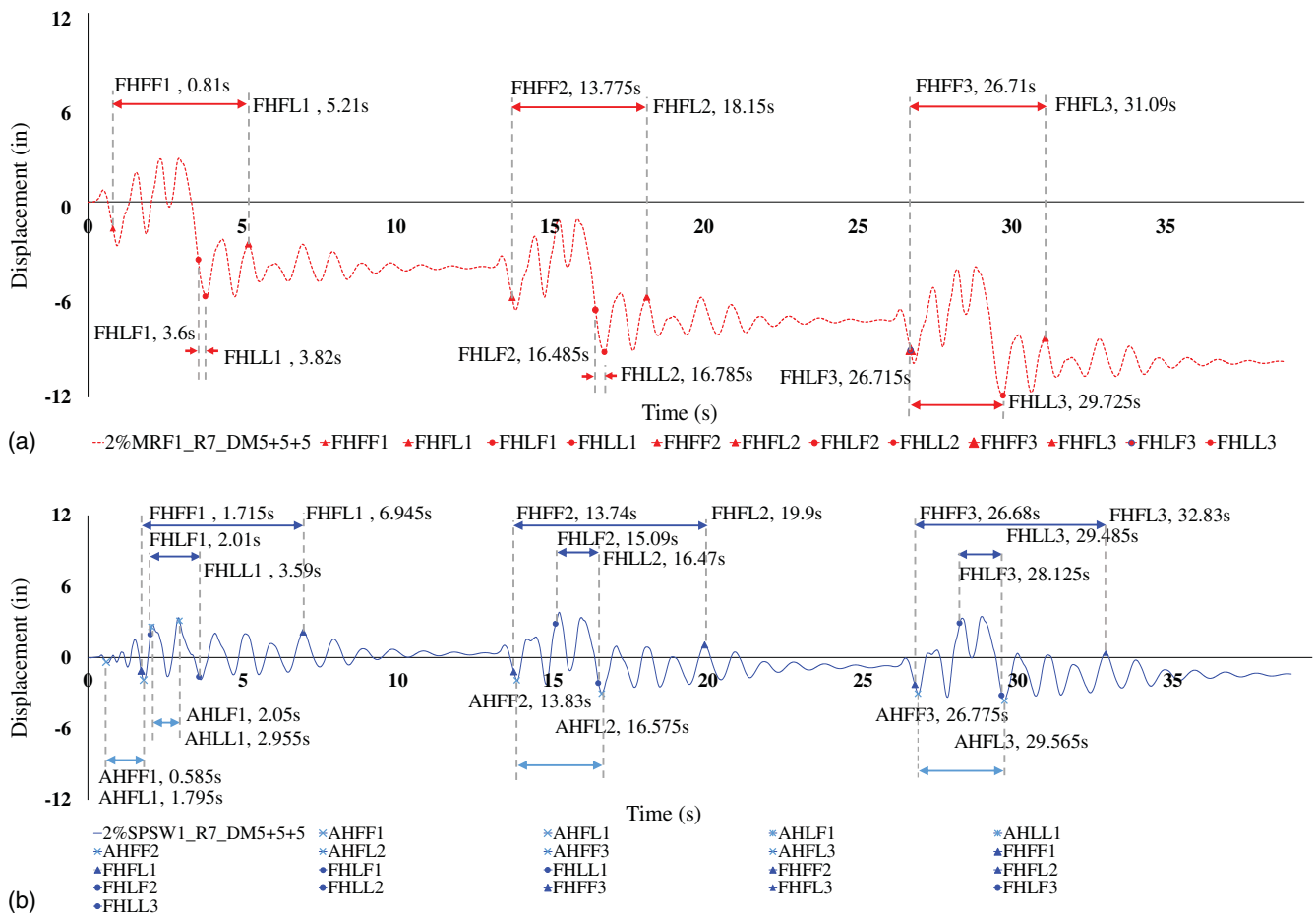


Fig. 8. Response history for case of DM5+5+5 with yield points for (a) MRF1; and (b) SPSW1.

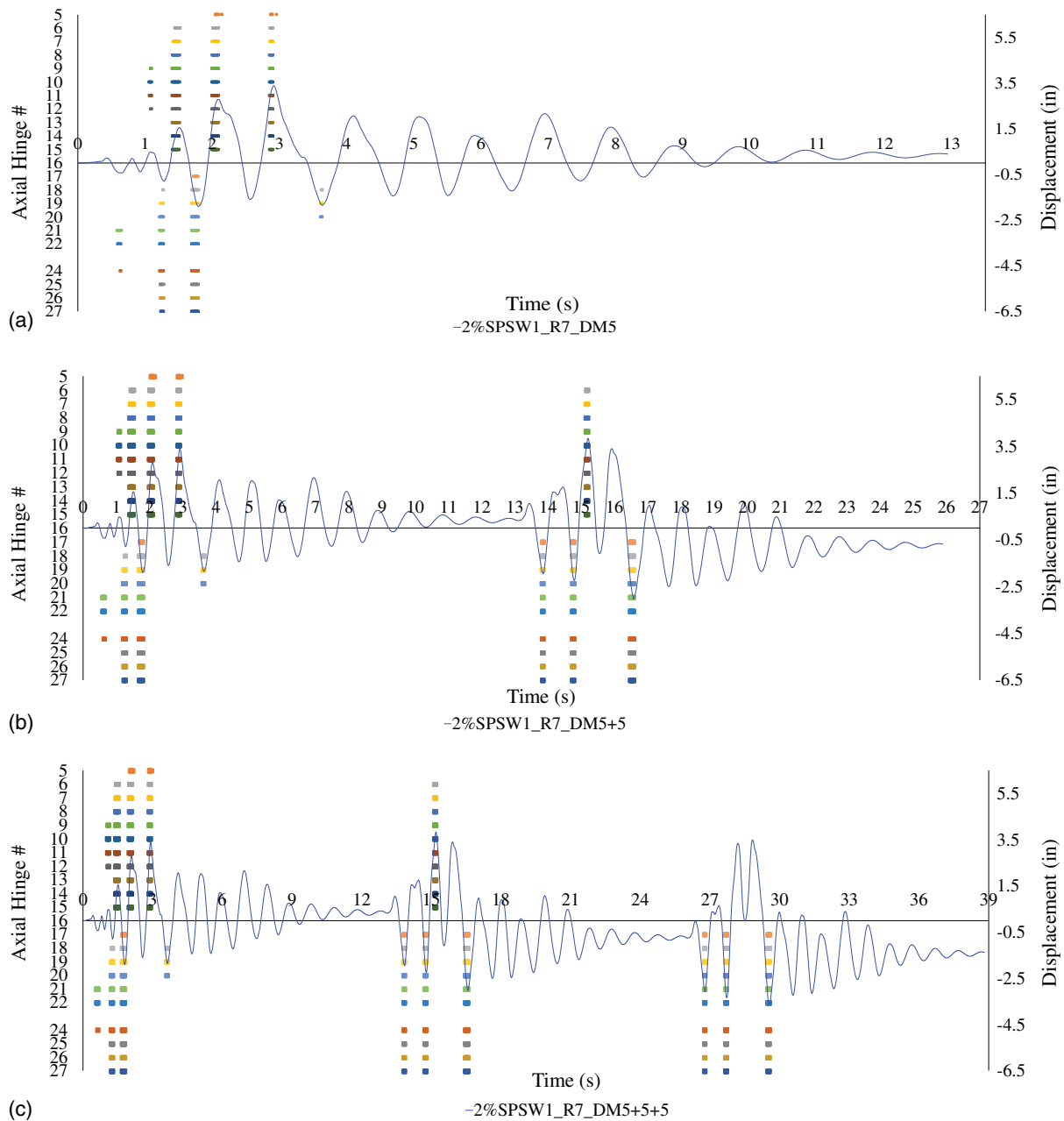


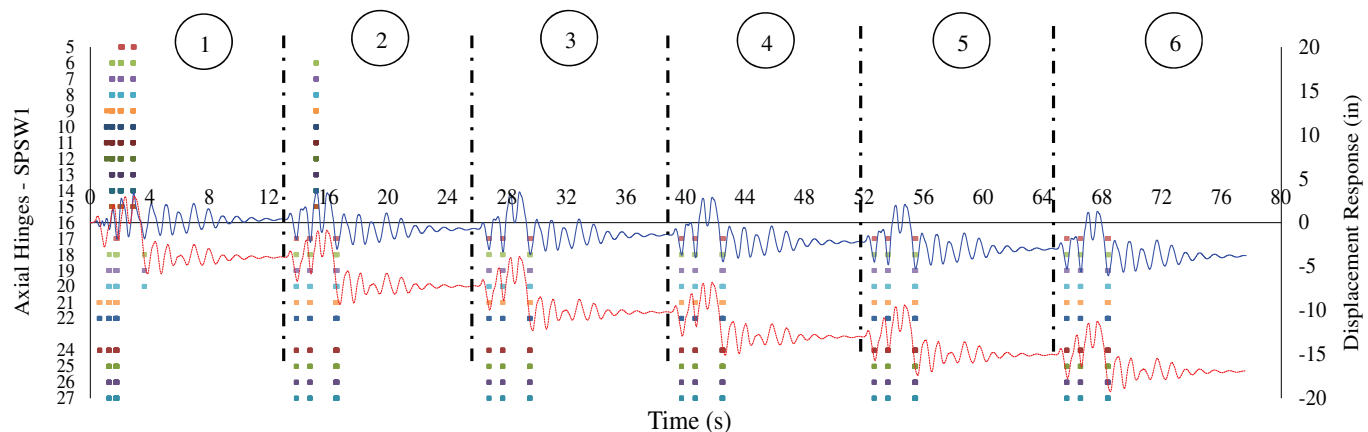
Fig. 9. Axial hinges yield bar charts for the cases of (a) DM5; (b) DM5+5; and (c) DM5+5+5.

cases. The primary vertical axis shows assigned axial hinge numbers for each strip (as per Fig. 5), whereas the secondary vertical axis depicts the HBE displacement in inches. Most of the axial hinges can be observed to have engaged readily in the first few cycles. The figure also shows that the structure had to undergo drift of value higher than the preceding peak for every subsequent yielding to occur. For the cases of DM5+5 and DM5+5+5, the strips continued to engage plastically, with response peaks corresponding to movements in the same direction as that of the residual drift for the entire system, causing instances of increased value of maximum drift. Therefore, the axial hinges were observed to repeat yielding for all such instances. However, response peaks in the direction opposite to the residual drift were seen to eventually cease to cause the corresponding strips to yield. This procedure helped in depicting the progression of plastic behavior of the steel plate, and accumulation of plastic strains, with the passage of time.

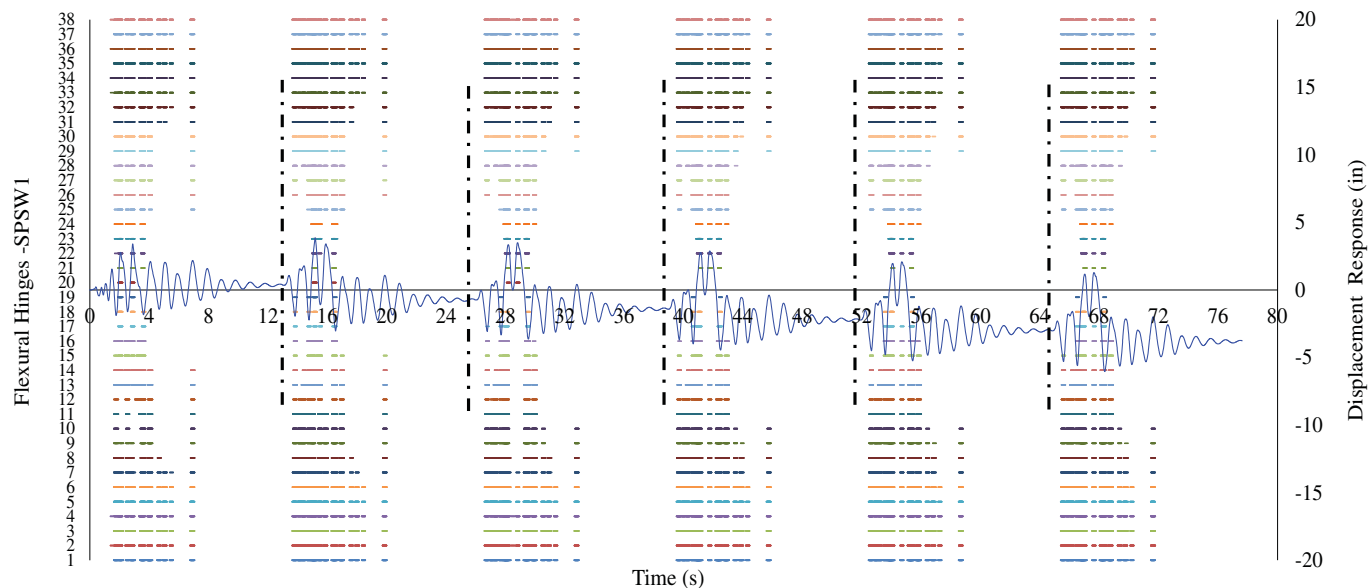
Cross Comparison of Overall Behavior

To achieve an overall understanding of the SPSW system, together with the respective contribution of each of its constituents, the previous approaches were condensed and plotted in one graph. For this purpose, the ground-motion time history was prolonged by repeating the DM5 record six times, with 4 s of intermittent zero padding between each consecutive synthetic record. This made the total duration of this case to be 78 s. Fig. 10(a) plots the yield behavior for SPSW1 axial hinges, along with SPSW1 flexural hinges in Fig. 10(b), which can be compared with the yield behavior of MRF1 flexural hinges in Fig. 10(c). For ease of visual inspection, the plots in Fig. 10 were divided into six segments of 13-s duration each. The first segment is presented in Fig. 11 for a zoomed-in, close-up version of the different yield behaviors observed.

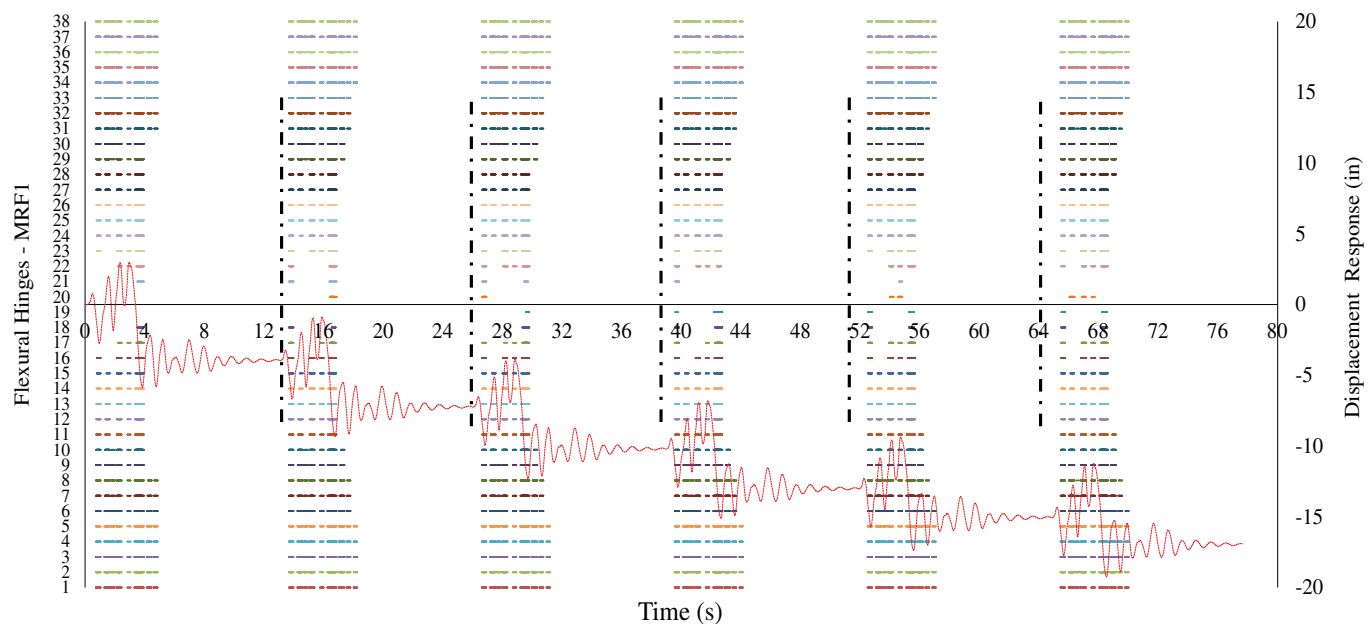
It can be noted from these figures that both MRF1 and SPSW1 engage in plastic behavior during the stronger portions of the



(a) -2%SPSW1_R7_DM5+5+5+5+5+5 -2%MRF1_R7_DM5+5+5+5+5+5



(b) -2%SPSW1_R7_DM5+5+5+5+5+5



(c) -2%MRF1_R7_DM5+5+5+5+5+5

Fig. 10. DM5+5+5+5+5 for $R = 7$, $\zeta = 2\%$, yield behavior for (a) SPSW axial hinges; (b) SPSW flexural hinges; and (c) MRF flexural hinges.

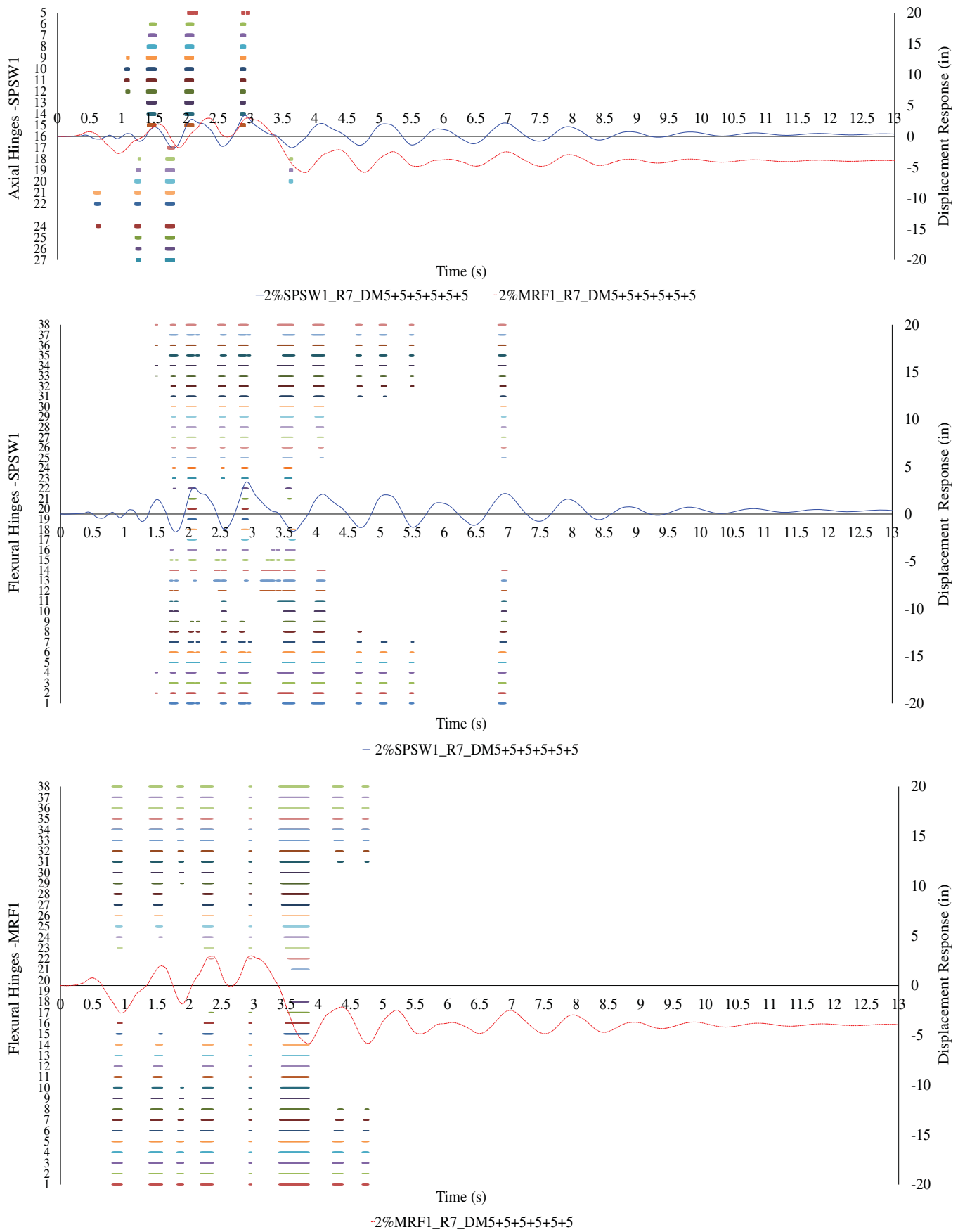


Fig. 11. SPSW1 yield behavior, Segment 1, 0 to 13 s.

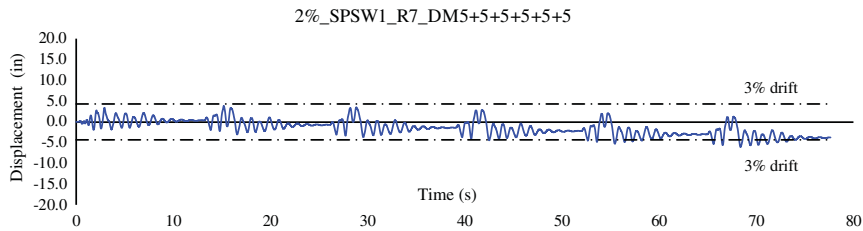


Fig. 12. SPSW1 displacement response for $\zeta = 2\%$, $R = 7$, DM5+5+5+5+5 with 3% drift mark.

ground motion. However, the response behavior was prominently different at the 7-s mark. A singular spike depicting yield within the flexural fiber hinges was observed for the SPSW1 response, whereas no such spike was seen at that time for the MRF1 response. The SPSW axial hinges were examined to understand the nature of this dissimilarity and to get an idea of the changes in stress conditions within the steel web with respect to time. It was noted that the axial hinges experienced plastic behavior approximately up to the 3.8-s mark, beyond which the stresses within the web did not undergo yielding due to the decrease in amplitude of the input ground motion. The ground acceleration amplitude continued to decrease up until the 7-s mark, where a slight increase was noted. This sudden increase in loading resulted in new stresses, but did not reengage the steel web further because, at that time, the value of the overall drift was less than previous yielding (at the 3.8-s mark). At this point the steel plate was considered prestretched and could not resist the sudden acceleration, leaving the boundary frame alone to account for it. The yielding spike noted earlier within the response was therefore a characteristic of the previous behavior. After this point, the SPSW1 model behaved as it would without a steel infill plate, up until the point where the overall drift became large enough to exceed levels previously produced. Then, the steel plate was observed to reengage, hence never acting identical to the MRF archetype. The MRF1 model experienced higher values of displacement response prior to this point, allowing it to drift without yielding, up until the next consecutive DM5 repetition. The bare boundary frame continued to yield progressively as the residual drifts accumulated with each consecutive peak of maximum drift.

It can be deduced from these observations that the steel plate continued to contribute strength to the system when subjected to long-duration ground motion. It delayed yielding of the boundary frame and limited increase in residual drifts for the structure by

catching the boundary frame at every successive point of maximum drift. During the times when the frame drift was less than the previous peak and the steel plate was effectively stretched or noncontributing, all of the seismic demand was resisted by the boundary frame, for which the HBE plays a major role in limiting drift. Design of the HBE section therefore becomes fundamental to overall seismic behavior of the SPSW system. Note that 3%–4% drift is understood to be a usual range for satisfactory seismic performance of SPSWs, but it can be seen from Fig. 12 that the SPSW1 displacement response exceeded the 3% drift mark after the fifth ground-motion repetition (after 52.6 s of total ground shaking—or 36.6 s after subtracting the padded zero acceleration segments). Although this research did not include the limit states of strength degradation, P -delta effects, and fracture, it can be seen that even without considering these detrimental effects that typically increase drifts, the SPSW would never behave as a bare frame owing to the accumulation of residual drift.

Moment Frame versus Gravity Frame

In order to investigate the possible role of the moment frame in limiting the SPSW from developing excessive increasing drifts, and eventually collapse during a long duration of shaking, analyses were conducted for a single-story SPSW system, but without moment connections. This SPSW was designed using the same beam and column sizes as SPSW1, but with the beams given pin connections at their ends. As was the case for SPSW1, this system took value of $R = 7$ and was analyzed for $\zeta = 2\%$ against six repetitions of the DM5 record. For comparison purposes, a gravity frame designed similar to the MRF system, but with pin connections, was also analyzed; it is denoted as GF. Fig. 13 presents response histories for the SPSW and GF, both with pin connections, along with

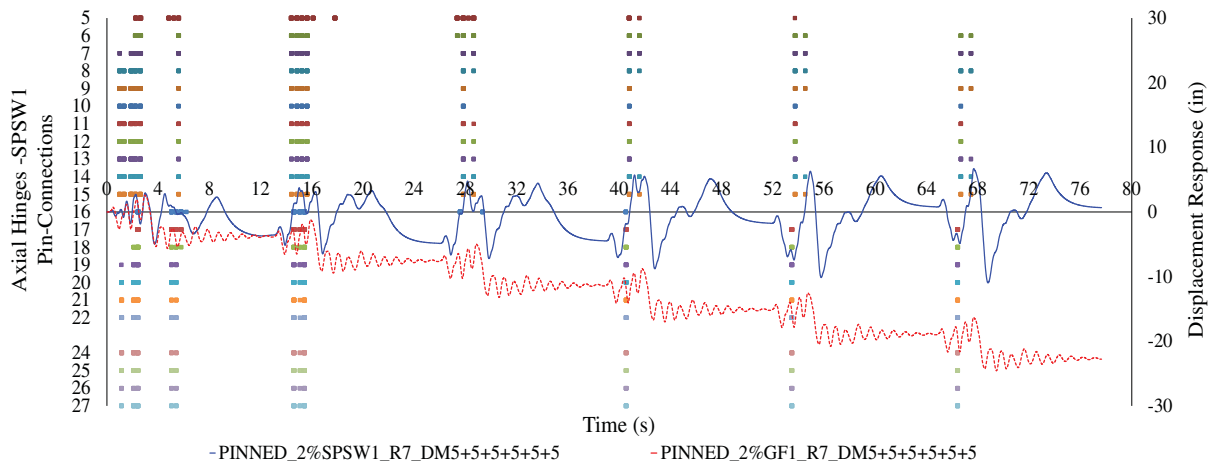


Fig. 13. Axial hinges yield behavior for 1:1 SPSW with pin connections for DM5+5+5+5+5 for $R = 7$, $\zeta = 2\%$.

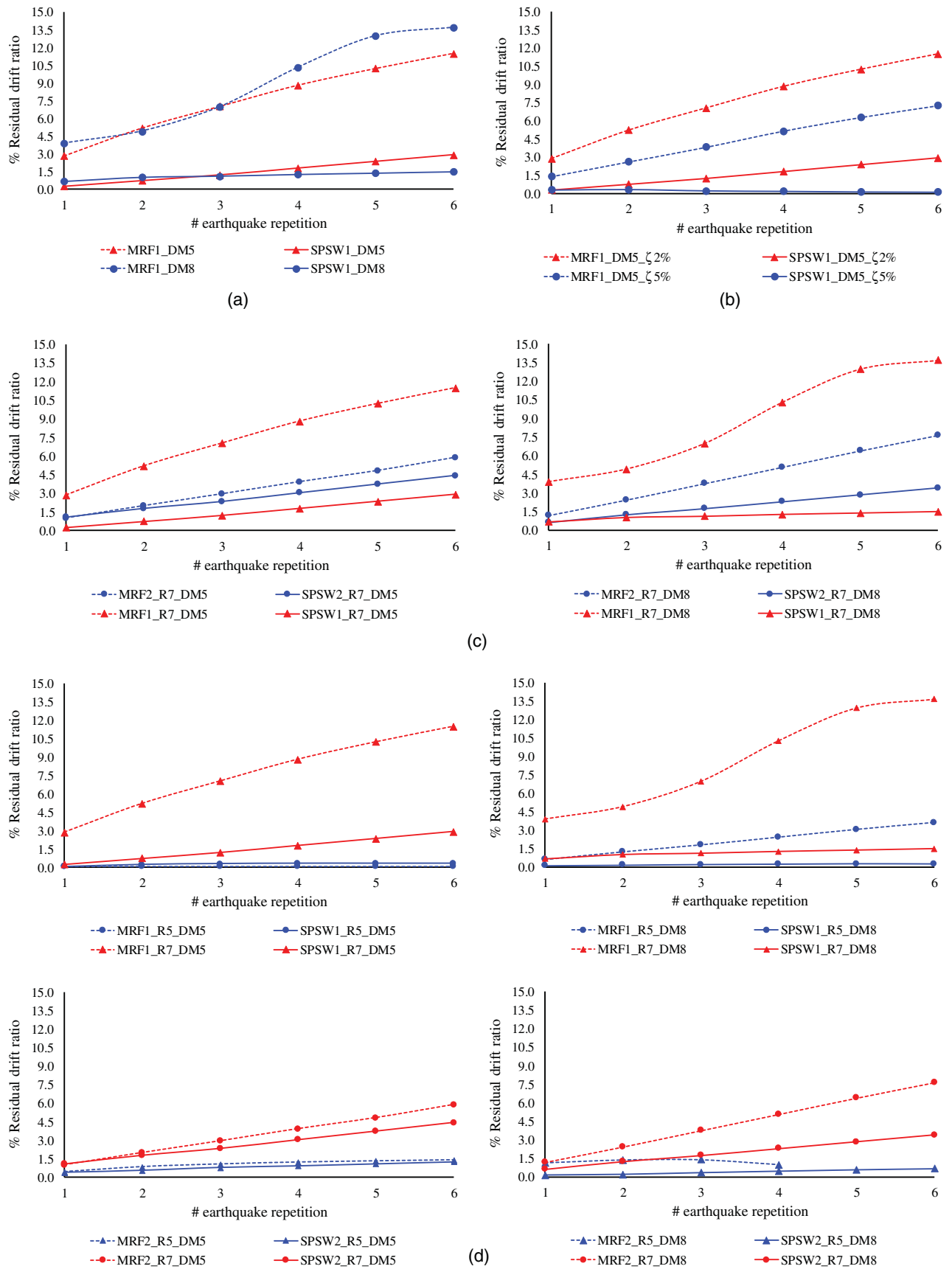


Fig. 14. Percentage residual drift with regard to increasing repetitions for (a) MRF1 and SPSW1 for DM5 and DM8; (b) MRF1 and SPSW1 designed for $\zeta = 2\%$ and $\zeta = 5\%$; (c) MRF2 and SPSW2 for DM5 and DM8; (d) MRF1 and SPSW1 designed for $R = 5$ and $R = 7$, for DM5 and DM8, and MRF2 and SPSW2 designed for $R = 5$ and $R = 7$, checked for DM5 and DM8; and (e) MRF3 and SPSW3 for $R = 7$, with regard to increasing DM5 repetitions for first floor, second floor, and top floor.

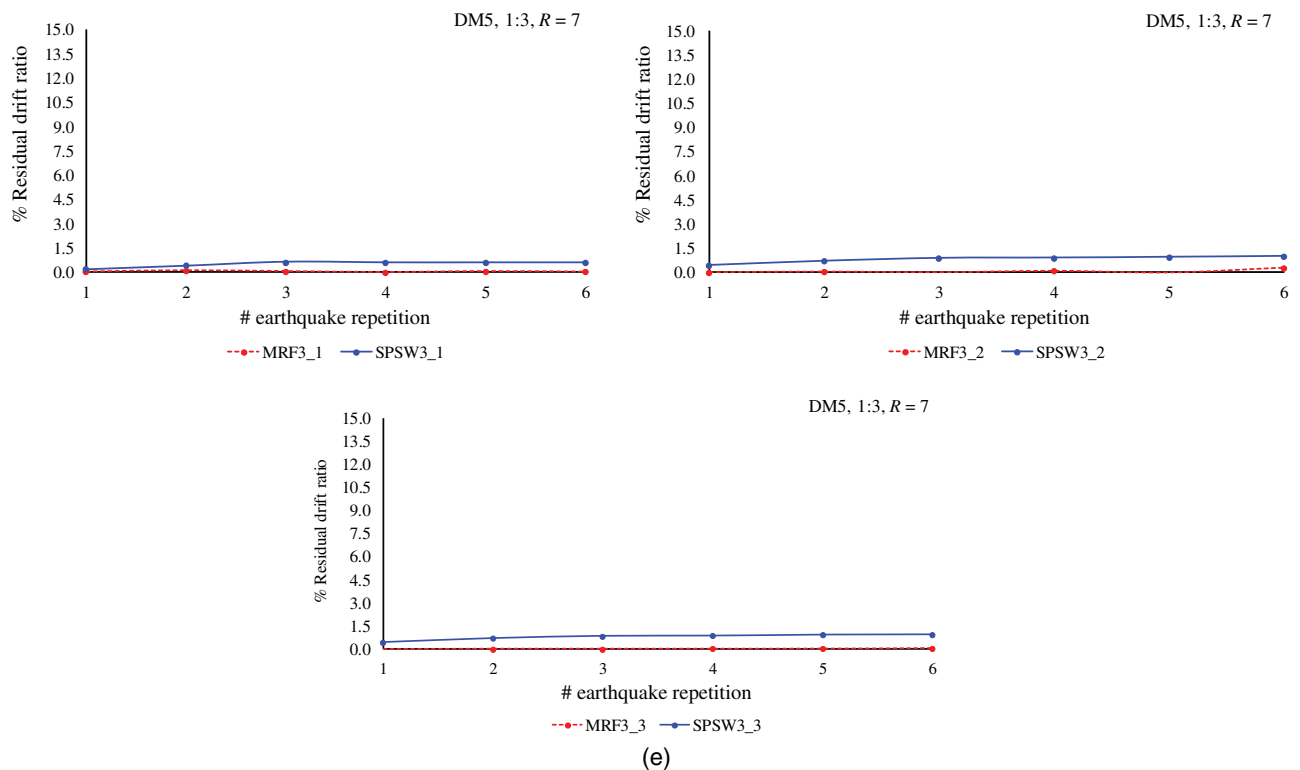


Fig. 14. (Continued.)

yielding behavior of the steel plate web. It can be seen that the SPSW model with such a configuration exceeded the 3% drift limit in just 3.6 s through the first DM5 magnitude record. As mentioned previously, the plastic plateau for each material model was taken as constant up to large strains, and therefore neither archetype was seen to reach total collapse (they just yield to excessive drifts). Without this modeling assumption, the SPSW with pinned connections would obviously drift incrementally to collapse more rapidly. However, in SPSWs, even simple beam–column connections (e.g., shear tab and/or double-angle connections) can develop some flexural strength and ductility due to the large axial and shear forces to be transferred at their ends resulting from tension force developing in the infill along the beams (e.g., Berman and Bruneau 2005). This contribution will expectedly vary as a function of SPSW aspect ratios, and quantifying this impact could be the subject of future research.

Sensitivity of Results Obtained

For SPSW1 designed for $R = 7$ and $\zeta = 2\%$, sensitivity to the increase in values of accumulated residual drift was noted and compared for multiple repetition sequences for ground motions DM5 and DM8. This comparison is detailed in Fig. 14(a) for both magnitudes considered. It can be observed that the residual drifts increase in both the SPSW and MRF cases, but the overall residual drift in the MRF, given its lesser stiffness, is of much higher value than that in the SPSW. The increase in residual drift for the MRF grew rapidly only after three repetitions of DM5 ground motion, and became gradually constant after. On the other hand, for the DM8 record, the increase in percent residual drift only reached a plateau during the last repetition. As was noted in previous sections, for the MRF the entire cross section for the HBE does not fully yield for the first few repetition sequences, and

therefore it only demonstrates a comparatively constant increase in drift when all fibers within the cross section are fully engaged. The SPSW, on the other hand, demonstrates a lesser rate of change in the additional residual drift with increasing duration. This is because the steel plate enables the HBE cross section to fully yield early on through the duration of the earthquake loading, allowing for the increase in residual drift to become a near-constant value after each ground motion repetition occurrence, straight from the beginning.

Next, sensitivity to the value of damping ratio was considered. For $R = 7$, the SPSW1 and MRF1 models were analyzed twice for the input time history of magnitude of DM5 with values of damping ratio ζ taken as 2% and 5% that of critical damping. Fig. 14(b) plots the increase in residual drift at each consecutive repetition for both values of damping considered. As can be seen, values of percentage residual drift for $\zeta = 5\%$ are less compared to those obtained for $\zeta = 2\%$. This is owing to the limited participation of the now more damped boundary frame and the reduced engagement of the steel web panel.

Similarly, the relationship trends between response of the system under prolonged durations and the dimensions of the steel infill were also considered, and are presented in Fig. 14(c). Here, the SPSW2, with aspect ratio of 2.0, has been compared with trends observed for SPSW1 in Fig. 14(a), and it can be seen that the SPSW2 showed a slightly higher accumulation of residual drift as compared to the SPSW1 archetype. However, the converse was true for the MRF archetypes, where relatively lesser values of addition to residual drift were observed for MRF2 as compared to MRF1. Yet, the previous observations in comparing MRF and SPSW results remain true.

Then, values of the response modification factor, R , were varied as 5 and 7 for both archetypes in order to investigate the variation of results with the ductility of the structure. Fig. 14(d) plots and compares variations in progressive residual drift accumulation

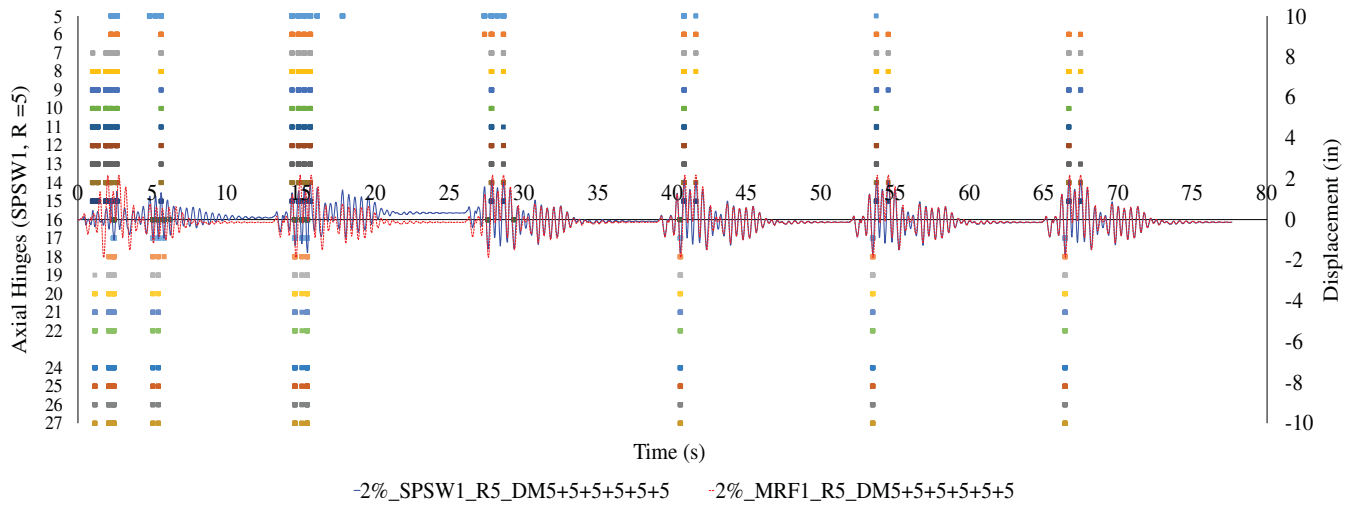


Fig. 15. Axial hinge yield behavior for SPSW1, $R = 5$, $\zeta = 2\%$ for DM5+5+5+5+5+5.

for SPSW1 and SPSW2, each designed for both these values of R , against six repetition sequences of DM5 and DM8 stochastic records, respectively. It can be seen that for decreasing values of R , the residual drift ratio generally decreased (as expected). The SPSW and the MRF both displayed negligible accumulation of residual drift for the case of SPSW1 with an R value of 5. Upon investigation of the displacement response, both the MRF and SPSW were observed to follow narrowly similar paths for the case of DM5. This is presented in Fig. 15 along with the yield behavior for the steel plate, from which it can be seen that the steel plate infill engaged extensively for the first two ground-motion repetitions, after which both archetypes fell into a similar pattern of displacement.

Also, the 3-story model, SPSW3, designed with value of $R = 7$, was analyzed with a value of $\zeta = 2\%$ in order to observe the sensitivity of results to increasing the number of stories in the structural system. Trends observed for story drift under DM5 repetitions are presented in Fig. 14(e). As can be seen from the figure, for the DM5 ground-motion repetitions, the MRF3 archetype does not seem to accumulate much residual drift relative to the SPSW3 structural system. Fig. 16 illustrates the response histories of each floor for both SPSW3 and MRF3, denoted by the model name followed by the floor number, e.g., SPSW3_1, MRF3_1. Comparison of these response histories shows that despite the SPSW3 showing a larger percentage residual drift, the MRF3 model has much higher values for maximum residual drift per repetition than those for

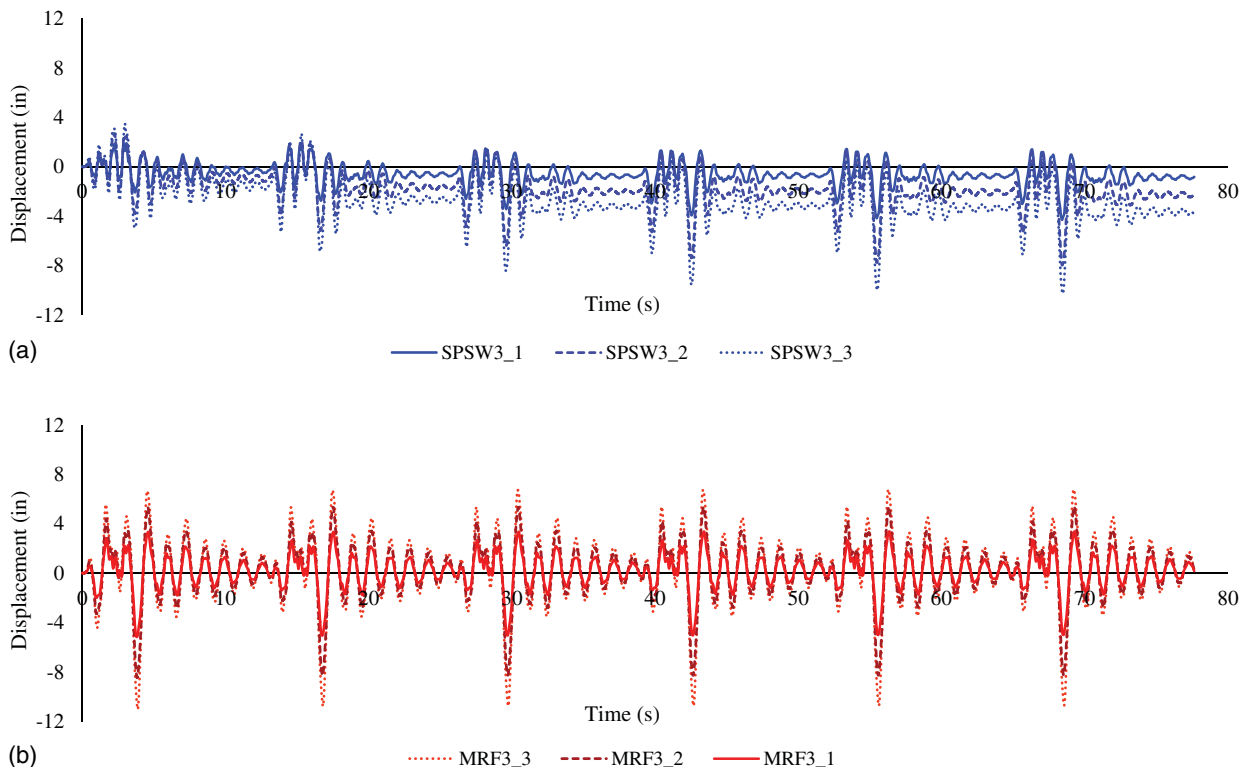


Fig. 16. Displacement response histories for all three stories for DM5 repetitions for (a) SPSW3; and (b) MRF3.

SPSW3. As presented in Fig. 16(a), the response oscillations show that the MRF3 behaves like a single-degree-of-freedom structure, and also does not appear to damp out quickly. Therefore, it can be said that the trends observed for the 3-story model followed those for the single story, even though the MRF3 archetype accumulated comparable residual drift relative to the SPSW3 model.

Conclusions

Analyses were conducted to understand the performance of SPSWs under long-duration synthetically generated ground motions. Analyses were conducted for the SPSWs as well as, for comparison, for their respective boundary frame alone (i.e., the SPSWs without their infill web plates). Trends in sensitivity of SPSW response for various configurations were plotted as a function of increasing duration of seismic loading. It was seen that despite the progressive increase in drift, the SPSW never reached a point where it behaved exactly like a simple moment-resisting frame corresponding to its own boundary frame. The presence of the steel plate infill limited the overall accumulation of residual drifts and restricted the boundary frame from drifting freely. It effectively delayed yielding of the boundary frame, and continued to provide strength and stability even after extensive exposure to strong ground motion.

Additionally, it was observed that the HBE members accounted for a significant part of the system's energy dissipation, even when the steel plate yielded beyond its preceding maximum elongation. Moment-resisting boundary elements were found to be instrumental for limiting drifts and preventing collapse for the system. SPSWs with pin-connected HBEs were observed to behave poorly. This illustrates the importance of providing substantial boundary frame members; in other words, moment-resisting connections are important to achieve appropriate performance of the SPSW structural system as a whole when subjected to earthquake loading (here, for the satisfactory responses observed, the boundary frames were sized to meet the ANSI/AISC 341-16 requirements).

Overall, the effects of increasing the duration of shaking were found to be less unfavorable for the SPSW than originally expected. A direct measure of the influence of ground-motion duration was the residual drift that accumulated during prolonged seismic loading. With increase in duration of earthquake excitation, slightly higher drifts were observed to accumulate for rectangular SPSWs with higher panel aspect ratios as compared to the bare frame. The residual displacements were seen to increase or decrease accordingly with the increasing or decreasing values of R when observed together with duration increase. For the multistory SPSW3, the trends observed followed those seen for the other models, but results showed lesser residual drifts when compared with those obtained for the single-story wall.

As a first step toward determining efficacy of the infill under long duration of excitation, this research considered infinitely ductile elastoplastic material properties, not taking into account effects of strain hardening, strength degradation, and P -delta effects. Further studies are necessary to understand the combined effect of these on SPSW behavior.

References

- AISC. 2016. *Seismic provisions for structural steel buildings*. ANSI/AISC 341-16. Chicago: AISC.
- ASTM. 2014. *Specification for carbon structural steel*. ASTM A36/A36M-14. West Conshohocken, PA: ASTM.
- ASTM. 2015. *Standard specification for structural steel shapes*. A992/A992M-11. West Conshohocken, PA: ASTM.
- Anjan, K. B., R. G. Driver, and G. Y. Grondin. 2009. "Seismic analysis of steel plate shear walls considering strain rate and P -delta effects." *J. Constr. Steel Res.* 65 (5): 1149–1159. <https://doi.org/10.1016/j.jcsr.2008.08.003>.
- ASCE. 2010. *Minimum design loads for buildings and other structures*. ASCE 7. Reston, VA: ASCE.
- Astaneh-Asl, A. 2001. *Seismic behavior and design of steel shear walls*. Steel TIPS Rep. Moraga, CA: Structural Steel Educational Council.
- Atkinson, G. M., and W. Silva. 2000. "Stochastic modeling of California ground motions." *Bull. Seismol. Soc. Am.* 90 (2): 255–274. <https://doi.org/10.1785/0119990064>.
- Berman, J., and M. Bruneau. 2003. "Plastic analysis and design of steel plate shear walls." *J. Struct. Eng.* 129 (11): 1448–1456. [https://doi.org/10.1061/\(ASCE\)0733-9445\(2003\)129:11\(1448\)](https://doi.org/10.1061/(ASCE)0733-9445(2003)129:11(1448)).
- Berman, J. W. 2011. "Seismic behavior of code designed steel plate shear walls." *Eng. Struct.* 33 (1): 230–244. <https://doi.org/10.1016/j.engstruct.2010.10.015>.
- Berman, J. W., and M. Bruneau. 2004. "Steel plate shear walls are not plate girders." *Eng. J. Am. Inst. Steel Constr.* 41 (3): 95–106.
- Berman, J. W., and M. Bruneau. 2005. "Experimental investigation of light-gauge steel plate shear walls." *J. Struct. Eng.* 131 (2): 259–267. [https://doi.org/10.1061/\(ASCE\)0733-9445\(2005\)131:2\(259\)](https://doi.org/10.1061/(ASCE)0733-9445(2005)131:2(259)).
- Berman, J. W., and M. Bruneau. 2008. "Capacity design of vertical boundary elements in steel plate shear walls." *Eng. J. Am. Inst. Steel Constr.* 45 (1): 55–71.
- Bommer, J. J., G. Magenes, J. Hancock, and P. Penazzo. 2004. "The influence of strong-motion duration on the seismic response of masonry structures." *Bull. Earthquake Eng.* 2 (1): 1–26. <https://doi.org/10.1023/B:BEEE.0000038948.95616.bf>.
- Borello, D. J., and L. A. Fahnestock. 2013. "Seismic design and analysis of steel plate shear walls with coupling." *J. Struct. Eng.* 139 (8): 1263–1273. [https://doi.org/10.1061/\(ASCE\)ST.1943-541X.0000576](https://doi.org/10.1061/(ASCE)ST.1943-541X.0000576).
- Borello, D. J., A. A. Quinonez, and L. A. Fahnestock. 2014. "Steel plate shear walls with coupling in high-seismic regions." In *Proc., 10th US National Conf. on Earthquake Engineering: Frontiers of Earthquake Engineering, NCEE 2014*. Oakland, CA: Earthquake Engineering Research Institute.
- Bruneau, M., and T. Bhagwagar. 2002. "Seismic retrofit of flexible steel frames using thin infill panels." *Eng. Struct.* 24 (4): 443–453. [https://doi.org/10.1016/S0141-0296\(01\)00111-0](https://doi.org/10.1016/S0141-0296(01)00111-0).
- Cao, C.-H., W.-H. Zhong, F. Li, J.-P. Hao, and Y.-C. Wang. 2007. "Cyclic test of diagonal stiffened steel plate shear walls." In *Proc., 10th Int. Symp. on Structural Engineering for Young Experts*, 437–442. Beijing: Science Press.
- Chandramohan, R., J. W. Baker, and G. G. Deierlein. 2016. "Quantifying the influence of ground motion duration on structural collapse capacity using spectrally equivalent records." *Earthquake Spectra* 32 (2): 927–950. <https://doi.org/10.1193/122813EQS298MR2>.
- Choi, I.-R., and H.-G. Park. 2009. "Steel plate shear walls with various infill plate designs." *J. Struct. Eng.* 35 (7): 785–796. [https://doi.org/10.1061/\(ASCE\)0733-9445\(2009\)135:7\(785\)](https://doi.org/10.1061/(ASCE)0733-9445(2009)135:7(785)).
- Choi, I.-R., and H.-G. Park. 2011. "Cyclic loading test for reinforced concrete frame with thin steel infill plate." *J. Struct. Eng.* 137 (6): 654–664. [https://doi.org/10.1061/\(ASCE\)ST.1943-541X.0000317](https://doi.org/10.1061/(ASCE)ST.1943-541X.0000317).
- Clayton, P. M., D. M. Dowden, C. H. Li, J. W. Berman, M. Bruneau, L. N. Lowes, and K. C. Tsai. 2016. "Self-centering steel plate shear walls for improving seismic resilience." *Front. Struct. Civ. Eng.* 10 (3): 283–290. <https://doi.org/10.1007/s11709-016-0344-z>.
- CSA (Canadian Standards Association). 2014. *Design of steel structures*. CSA S16. Toronto: CSA.
- Dastfan, M., and R. G. Driver. 2008. "Flexural stiffness limits for frame members of steel plate shear wall systems." In *Proc., Annual Stability Conf.*. Rolla, MO: Structural Stability Research Council.
- Driver, R. G., G. L. Kulak, A. E. Elwi, and D. J. L. Kennedy. 1998a. "FE and simplified models of steel plate shear wall." *J. Struct. Eng.* 124 (2): 121–130. [https://doi.org/10.1061/\(ASCE\)0733-9445\(1998\)124:2\(121\)](https://doi.org/10.1061/(ASCE)0733-9445(1998)124:2(121)).
- Driver, R. G., G. L. Kulak, D. J. L. Kennedy, and A. E. Elwi. 1998b. "Cyclic test of four-story steel plate shear wall." *J. Struct. Eng.*

- 124 (2): 112–120. [https://doi.org/10.1061/\(ASCE\)0733-9445\(1998\)124:2\(112\)](https://doi.org/10.1061/(ASCE)0733-9445(1998)124:2(112)).
- Elgaaly, M., V. Caccese, and C. Du. 1993. “Postbuckling behavior of steel-plate shear walls under cyclic loads.” *J. Struct. Eng.* 119 (2): 588–605. [https://doi.org/10.1061/\(ASCE\)0733-9445\(1993\)119:2\(588\)](https://doi.org/10.1061/(ASCE)0733-9445(1993)119:2(588)).
- Elgaaly, M., and Y. Liu. 1997. “Analysis of thin-steel-plate shear walls.” *J. Struct. Eng.* 123 (11): 1487–1496. [https://doi.org/10.1061/\(ASCE\)0733-9445\(1997\)123:11\(1487\)](https://doi.org/10.1061/(ASCE)0733-9445(1997)123:11(1487)).
- Hou, H., and B. Qu. 2015. “Duration effect of spectrally matched ground motions on seismic demands of elastic perfectly plastic SDOFS.” *Eng. Struct.* 90: 48–60. <https://doi.org/10.1016/j.engstruct.2015.02.013>.
- Hou, H., and B. Qu. 2016. “Influence of cumulative damage on seismic response modification factors of elastic perfectly plastic oscillators.” *Adv. Struct. Eng.* 19 (3): 473–487. <https://doi.org/10.1177/1369433216630119>.
- Housner, G. W. 1965. “Intensity of ground motion shaking near the causative fault.” In *Proc., 3rd World Conf. on Earthquake Engineering*, 94–109. Canberra, Australia: Bureau of Mineral Resources, Geology and Geophysics, Dept. of National Development.
- Iervolino, I., G. Manfredi, and E. Cosenza. 2006. “Ground motion duration effects on nonlinear seismic response.” *Earthquake Eng. Struct. Dyn.* 35 (1): 21–38. <https://doi.org/10.1002/eqe.529>.
- Kawashima, K., and K. Aizawa. 1989. “Bracketed and normalized durations of earthquake ground acceleration.” *Earthquake Eng. Struct. Dyn.* 18 (7): 1041–1051. <https://doi.org/10.1002/eqe.4290180709>.
- Kawashima, K., and Takahashi, K. 1985. “Duration of strong motion acceleration records.” In *Proc., Japan Society of Civil Engineers 1985*, 161–168. Tokyo: Japan Society of Civil Engineers.
- Kojima, K., and I. Takewaki. 2015. “Critical input and response of elastic-plastic structures under long-duration earthquake ground motions.” *Front. Built Environ.* 1: 15. <https://doi.org/10.3389/fbuil.2015.00015>.
- Lignos, D. G., Y. Chung, T. Nagae, and M. Nakashim. 2011. “Numerical and experimental evaluation of seismic capacity of high-rise steel buildings subjected to long duration earthquakes.” *Comput. Struct.* 89 (11–12): 959–967. <https://doi.org/10.1016/j.compstruc.2011.01.017>.
- Lubell, A. S., H. G. Prion, C. E. Ventura, and M. Rezaei. 2000. “Unstiffened steel plate shear wall performance under cyclic loading.” *J. Struct. Eng.* 126 (4): 453–460. [https://doi.org/10.1061/\(ASCE\)0733-9445\(2000\)126:4\(453\)](https://doi.org/10.1061/(ASCE)0733-9445(2000)126:4(453)).
- Mantawy, A., and J. Anderson. 2018. “Effect of long-duration earthquakes on the low-cycle fatigue damage in RC frame buildings.” *Soil Dyn. Earthquake Eng.* 109: 46–57. <https://doi.org/10.1016/j.soildyn.2018.01.013>.
- Marafi, N. A., J. W. Berman, and M. O. Eberhard. 2016. “Ductility-dependent intensity measure that accounts for ground-motion spectral shape and duration.” *Earthquake Eng. Struct. Dyn.* 45 (4): 653–672. <https://doi.org/10.1002/eqe.2678>.
- Marsh, M. L., and Gianotti, C. M. 1994. *Structural response to long-duration earthquakes*. WA-RD 340.2. Pullman, WA: Washington State Transportation Center.
- Papageorgiou, A., and B. Halldorsson. 2004. *Response spectrum compatible time histories*. Buffalo, NY: State Univ. of New York at Buffalo.
- Park, H.-G., J.-H. Kwack, S.-W. Jeon, W.-K. Kim, and I.-R. Choi. 2007. “Framed steel plate wall behavior under cyclic lateral loading.” *J. Struct. Eng.* 133 (3): 378–388. [https://doi.org/10.1061/\(ASCE\)0733-9445\(2007\)133:3\(378\)](https://doi.org/10.1061/(ASCE)0733-9445(2007)133:3(378)).
- Purba, R., and M. Bruneau. 2015. “Seismic performance of steel plate shear walls considering two different design philosophies of infill plates. I: Deterioration model development.” *J. Struct. Eng.* 141 (6): 04014160. [https://doi.org/10.1061/\(ASCE\)ST.1943-541X.0001098](https://doi.org/10.1061/(ASCE)ST.1943-541X.0001098).
- Qu, B., M. Bruneau, C.-H. Lin, and K.-C. Tsai. 2008. “Testing of full-scale two-story steel plate shear wall with reduced beam section connections and composite floors.” *J. Struct. Eng.* 134 (3): 364–373. [https://doi.org/10.1061/\(ASCE\)0733-9445\(2008\)134:3\(364\)](https://doi.org/10.1061/(ASCE)0733-9445(2008)134:3(364)).
- Rezaei, M. 1999. “Seismic behaviour of steel plate shear walls by shake table testing.” Ph.D. thesis, Dept. of Civil Engineering, Univ. of British Columbia.
- Sabouri-Ghomi, S., C. E. Ventura, and M. H. K. Kharrazi. 2005. “Shear analysis and design of ductile steel plate walls.” *J. Struct. Eng.* 131 (6): 878–889. [https://doi.org/10.1061/\(ASCE\)0733-9445\(2005\)131:6\(878\)](https://doi.org/10.1061/(ASCE)0733-9445(2005)131:6(878)).
- Thorburn, L. J., G. L. Kulak, and C. J. Montgomery. 1983. *Analysis of steel plate shear walls*. Edmonton, AB, Canada: Univ. of Alberta.
- Tirca, L., and Tremblay, R. 2004. “Influence of building height and ground motion type on the seismic behavior of zipper concentrically braced steel frames.” In *Proc., 13th World Conf. on Earthquake Engineering*. Vancouver, BC, Canada: Canadian Association for Earthquake Engineering.
- Trifunac, M. D., and A. G. Brady. 1975. “A study of the duration of strong earthquake ground motion.” *Bull. Seismol. Soc. Am.* 65 (3): 581–626. University of Washington. 2018. “The M9 project.” Natural Hazards. Accessed June 25, 2018. <https://hazards.uw.edu/geology/m9/>.
- USGS. 2014. “US seismic design maps.” U.S. Geological Survey, Earthquake Hazards Program. Accessed March 27, 2018. <https://earthquake.usgs.gov/designmaps/us/application.php>.
- Vanmarcke, E. H., and S.-S. Lai. 1980. “Strong-motion duration and RMS amplitude of earthquake records.” *Bull. Seismol. Soc. Am.* 70 (4): 1293–1307.
- Xie, L.-L., and X. Zhang. 1988. “Engineering duration of strong motion and its effects on seismic damage.” In *Proc., 9th World Conf. on Earthquake Engineering*, 307–312. Hoboken, NJ: Wiley.